Int. J. Heat Mass Transfer. Vol. 26, No. 6, pp. 871–880, 1983
Printed in Great Britain

0017-9310/83/060871-10 $03.00/0
Pergamon Press Ltd.

THERMAL PERFORMANCE OF RADIATIVE COOLING PANELS

P. BERDAHL, M. MARTIN and F. SAKKAL*
Lawrence Berkeley Laboratory, University of California, Berkeley, CA 94720, U.S.A.

(*Received* 29 *June* 1982 *and in final form* 21 *October* 1982)

Abstract—The performance of panels which cool by means of thermal infrared heat transfer to the sky is calculated from basic principles. The efficiency of a radiative cooling panel is defined. Computer calculations with the full heat transfer equations are performed for horizontal surfaces with infrared-transparent covers. Plots of efficiency versus a dimensionless temperature difference are shown to be insensitive to variations in air temperature, wind speed, and sky radiance, resulting in plots analogous to standard efficiency curves for solar panels. Experimental measurements show that, for most applications, white paint is a better radiator than aluminized polyvinyl fluoride film.

NOMENCLATURE

$B_a(\lambda)$, Planck blackbody function (per unit solid angle) at absolute temperature T_a (subscripts c and r correspond to temperatures T_c and T_r);
b, function of ε_s, equation (14);
C, normalization parameter in equation (14);
d, film thickness;
h, non-radiative heat transfer coefficient;
m, $1/\cos\theta$;
N, net cooling rate;
n, index of refraction;
$R_s(\theta, \lambda)$, thermal spectral radiance of the sky;
r, reflectance;
$\mathscr{R}$, Fresnel reflectance, equation (15);
S, total thermal sky radiance;
T, temperature;
t, transmittance.

Greek symbols

$\alpha(\lambda)$, spectral absorption coefficient;
ΔT_r, $T_a - T_r$;
ε, emissivity;
η, efficiency;
θ, zenith angle and angle of incidence;
θ', angle of incidence in a medium with index of refraction n;
λ, wavelength;
σ, Stefan–Boltzmann constant;
τ, dimensionless temperature difference, equation (10).

Subscripts

a, air;
c, cover;
dp, dewpoint;
max, maximum;
r, radiator;
s, sky.

Other symbols

$\oint_\Phi$, integration operator, equation (4).

* Present address: Dept. of Mech. Eng., American University, Beirut, Lebanon.

1. INTRODUCTION

THE ATMOSPHERE is not in radiative thermal equilibrium, and consequently objects exposed to the night sky cool spontaneously below air temperature. If an object has a solar reflectivity in excess of 95%, and if its thermal emissivity is not too small, it will also cool during the day. This cooling effect has the potential to displace energy used for the cooling of buildings if suitable systems can be developed. Pioneering work in this area has been done by Hay and Yellot [1, 2], Bliss [3], Head [4], Trombe [5], and Catalanotti *et al.* [6].

The amount of thermal sky radiation depends on the air temperature, dewpoint temperature, and cloud cover. Maximum cooling rates for radiators at air temperature occur under conditions of high air temperature, low dewpoint temperature, and no cloud cover. The presence of clouds can be unimportant if they are high (cold) and thin, as for example with cirrus clouds. However, for very low opaque clouds the radiative cooling effect is eliminated because the sky radiance is that of a blackbody at air temperature. For clear nocturnal sky conditions the sky radiance S can be estimated as

$$S = \varepsilon_s \sigma T_a^4 \tag{1}$$

where T_a is the absolute air temperature near the ground and the *apparent* sky emissivity at night is given by [7]

$$\varepsilon_s = 0.741 + 0.0062\, T_{dp}, \tag{2}$$

with T_{dp} the dewpoint temperature in °C.

The *distribution* of sky radiance with respect to both zenith angle and wavelength is non-uniform. The portion of the sky near the horizon has an effective radiative temperature equal to the air temperature near the ground. Also, outside the 8–13 μm portion of the spectrum, the atmosphere emits much like a blackbody at air temperature. Thus the resource for radiative

cooling is caused by the relative absence of thermal radiation from the zenith region of the sky in the 8–13 μm portion of the spectrum.

The quantitative evaluation of the performance of a cooling panel requires measurements of the thermal sky radiance. In a typical cooling experiment the thermal sky radiance may be 350 W m^{-2} with the panel emitting 420 W m^{-2}. An uncertainty of 10% in the 70 W m^{-2} of net cooling requires an accuracy of 2% in the measurement of the sky radiance, which can be achieved only by careful measurements under controlled conditions.

A number of recent experimental studies [8–30] have concentrated on horizontal radiator plates, insulated on the bottom and sides, covered by a polyethylene film as a convection shield. In some cases the polyethylene film contained pigments or a coating to reflect and/or absorb solar radiation [8–13]. Also, selectively emitting surfaces have been used as radiators [4–6, 8–17, 19, 20, 28–30] in addition to non-selective (black) surfaces such as ordinary paints. These selective surfaces have high emissivity in the 8–13 μm 'window' of the atmosphere in which the thermal sky radiation is weak, and low emissivity in the rest of the range of thermal wavelengths (5–40 μm). This selectivity permits larger cooling rates at low temperatures, thus lowering the minimum temperatures which can be achieved. The selective surface most often used is polyvinyl fluoride (PVF) 12 μm thick, aluminized on the underside. Our experimental work and analysis will show it to be inferior, in most applications, to simple white paint. It is hoped that better selective emitters can be developed.

In the next section we analyze the heat transfer from an uncovered radiator surface and define the concept of efficiency for radiative cooling. Section 3 gives the fully detailed heat transfer equations for a covered radiator. In Section 4, approximate techniques are presented for estimating the angular and spectral properties of the atmosphere ('sky'), windscreen cover, and radiator. Section 5 exhibits numerical results from the complete model defined by Sections 3 and 4, for selective and non-selective radiators below polyethylene windscreens. In Section 6 we compare the numerical results with our measured values of cooling efficiency and confirm the adequacy of the model.

2. RADIATIVE HEAT EXCHANGE WITH AN UNCOVERED RADIATOR

For simplicity, we initially consider the radiative heat transfer from a horizontal radiator without a cover. We also neglect the non-radiative heat transfer. The equations derived in this section will be relevant to real exposed surfaces if heat conduction, convection, and solar radiation are also included. The equations are also of approximate relevance to the case in which convection and conduction have been suppressed with a suitable cover glazing and back insulation, with only minimal impact on thermal infrared transfer.

The net steady-state cooling rate N (W m^{-2}) is given by

$$N = \oint \varepsilon_r(0,\lambda)[B_r(\lambda) - R_s(0,\lambda)] \tag{3}$$

where $\varepsilon_r(0,\lambda)$ is the radiator emissivity, B_r is the Planck function for the spectral radiance of a blackbody with absolute (radiator) temperature T_r (W m^{-2} sr^{-1} μm^{-1}), and R_s is the spectral radiance of the atmosphere. The integration operator $\oint$ is used here to abbreviate the appropriate integrations over wavelength λ and zenith angle θ

$$\oint = 2\pi \int_0^\infty d\lambda \int_0^1 \cos\theta \, d\cos\theta. \tag{4}$$

The radiator emissivity is assumed to be dependent on zenith angle but independent of azimuth angle. For most simple surfaces this is a good assumption. The sky radiance $R_s(0,\lambda)$ is also assumed independent of azimuth angle. This is quite a good assumption on the average, although for partly cloudy skies it is not true on an instantaneous basis. The absorptivity of the radiator has been eliminated from equation (3) by the use of Kirchhoff's law. The spectral and angular (apparent) sky emissivity is defined by

$$\varepsilon_s(0,\lambda) = R_s(0,\lambda)/B_a(\lambda) \tag{5}$$

where $B_a(\lambda)$ is the Planck function corresponding to T_a, the absolute air temperature. The sky emissivity obeys the equation

$$\frac{\oint B_a(\lambda)\varepsilon_s(0,\lambda)}{\oint B_a(\lambda)} = \varepsilon_s, \tag{6}$$

which shows that the integrated sky emissivity ε_s is the appropriate thermal average of $\varepsilon_s(0,\lambda)$. With equations (5) and (3), one has for the cooling power,

$$N = \oint \varepsilon_r(0,\lambda)[1-\varepsilon_s(0,\lambda)]B_a(\lambda) - \oint \varepsilon_r(0,\lambda)[B_a(\lambda) - B_r(\lambda)]. \tag{7}$$

The first term in this equation specifies the cooling power for the case $T_r = T_a$, that is, when the radiator is maintained at air temperature. It represents the cooling power available because the radiative 'temperature' of the sky is lower than the air temperature. Note that $\varepsilon_s(0,\lambda) = 1$ except for λ in the 8–13 μm window. Thus it is only the 8–13 μm values of $\varepsilon_r(0,\lambda)$ which are important in this term. The second term in equation (7) specifies the reduction in the cooling power when the radiator falls below air temperature. Note that the variation of N as a function of $\Delta T_r = T_a - T_r$ does not depend on the radiative properties of the sky as expressed by $\varepsilon_s(0,\lambda)$, but only upon the emissivity of the radiator.

For a given set of atmospheric conditions and radiator temperature there is an optimum radiator emissivity $\varepsilon_r(0,\lambda)$. Equation (3) shows that the optimum is $\varepsilon_r(0,\lambda) = 1$ if $B_r(\lambda) > R_s(0,\lambda)$, and zero otherwise. For

radiators above air temperature blackbody radiators are most efficient. However, for cooling below air temperature ($T_r < T_a$), selective emitters are more efficient. An ideal emitter for $T_r < T_a$ would be selective in angle as well as wavelength. For $T_a - T_r = 20°C$, the emitter should be emissive from 8 to 12.5 μm, for zenith angles of 0–70°, and reflective ($\varepsilon_r = 0$) otherwise. These numerical values are for typical clear midlatitude summer sky conditions [7].

The maximum cooling power is a diminishing function of $\Delta T_r = T_a - T_r$. Thus the maximum available cooling at any $\Delta T_r \geqslant 0$ occurs at $\Delta T_r = 0$. The value of this maximum is

$$N_{max} = \oint [1 - \varepsilon_s(0, \lambda)] B_a(\lambda) = (1 - \varepsilon_s)\sigma T_a^4. \quad (8)$$

The quantity N_{max} is system independent and consequently natural for use in forming the definition of efficiency,

$$\eta = \frac{N}{N_{max}} = \frac{N}{(1-\varepsilon_s)\sigma T_a^4}, \quad (9)$$

which is strictly less than unity provided $T_r < T_a$. In what follows it will also be useful to employ a dimensionless temperature difference,

$$\tau = \frac{4(T_a - T_r)}{(1-\varepsilon_s)T_a}. \quad (10)$$

Plots of η vs τ will be used to characterize different radiator panels. A Taylor's expansion of η,

$$\eta = \eta_0 + \eta_1\tau + \eta_2\tau^2 + \ldots,$$

can usually be terminated after the first two terms due to the smallness of the quantity $(T_a - T_r)/T_a$. For the case of the exposed radiator [equation (7)], η_1 is independent of variations in sky emissivity and η_0 is insensitive to such variations in many cases of interest. For example, if $\varepsilon_r(0, \lambda)$ is a constant for λ within the 8–13 μm range, then η_0 is independent of the sky emissivity.

3. HEAT EXCHANGE WITH A COVERED RADIATOR

The derivation of the heat transfer equations for a radiator with an infrared-transparent cover is more complex than for an exposed radiator but is still straightforward. The spectral and angular transmittance, emittance, and reflectance of the cover are denoted by $t_c(0, \lambda)$, $\varepsilon_c(0, \lambda)$ and $r_c(0, \lambda)$. The sum of these quantities is unity. The reflectance $r_c(0, \lambda)$ is taken as equal from above and below. The reflectance of the cover (and of the radiator) is assumed specular; that is, reflections do not alter the zenith angle 0 of the radiation. As before, we ignore any effects due to solar radiation. Let h_{ra} be the conduction coefficient for heat flow through the back insulation (radiator-to-air), h_{rc} be the conduction/convection coefficient between radiator and cover, and let h_{ca} be the conduction/convection coefficient from cover to ambient air.

With these assumptions and definitions, the net radiative heat loss N of the radiator, at equilibrium, is given by

$$N = \oint \left[\frac{t_c(0,\lambda)\varepsilon_r(0,\lambda)}{1 - r_r(0,\lambda)r_c(0,\lambda)}\right][B_r(\lambda) - R_s(0,\lambda)] + \oint \left[\frac{\varepsilon_c(0,\lambda)\varepsilon_r(0,\lambda)}{1 - r_r(0,\lambda)r_c(0,\lambda)}\right][B_r(\lambda) - B_c(\lambda)] + h_{ra}(T_r - T_a) + h_{rc}(T_r - T_c). \quad (11)$$

The denominators in this equation arise from multiple reflections between cover and radiator. The temperature of the cover, T_c, is determined from the cover heat balance assuming it has zero heat capacity,

$$\oint \left[\varepsilon_c(0,\lambda) + \frac{t_c(0,\lambda)\varepsilon_c(0,\lambda)r_r(0,\lambda)}{1 - r_r(0,\lambda)r_c(0,\lambda)}\right][B_c(\lambda) - R_s(0,\lambda)] + \oint \left[\frac{\varepsilon_c(0,\lambda)\varepsilon_r(0,\lambda)}{1 - r_r(0,\lambda)r_c(0,\lambda)}\right][B_c(\lambda) - B_r(\lambda)] + h_{rc}(T_c - T_r) + h_{ca}(T_c - T_a) = 0. \quad (12)$$

These equations are exact, except for the assumption that the polarization of the radiation is not important. For the cases of interest to us, the radiator emissivity is to a good approximation independent of polarization. Also, multiple reflections between radiator and cover are not too important, and, the thermal sky radiance is unpolarized. Therefore, it is sufficient to take the cover transparency and reflectivity as average values for the two polarizations.

It would be desirable to further simplify equations (11) and (12) by use of the usual hemispherical emissivities, eliminating the integrations over 0. However, this simplification is not allowed due to correlations among the various angular dependences. For example, in the first term in equation (11), each of the factors $t_c(0, \lambda)$, $\varepsilon_r(0, \lambda)$, and $R_s(0, \lambda)$ may have substantial variation with 0. Suppose $\varepsilon_r(0, \lambda) = 1$. The cover transparency $t_c(0, \lambda)$ will generally decrease with increasing 0. The sky radiance $R_s(0, \lambda)$ will increase with increasing 0. As a result the average value of the product $t_c(0, \lambda)R_s(0, \lambda)$ will be smaller than the product of the averages. The use of hemispherically averaged quantities in this case would lead to underestimates of the radiative cooling effect.

Equations (11) and (12) are in agreement with our earlier work [28, 29] and with that of others [8, 10] but disagree with those of Landro and McCormick [17]. It is difficult to assess the accuracy of their equation (6) since the radiator has been assumed to be both Lambertian [$\varepsilon_r(0, \lambda)$ independent of 0], and later to satisfy $\varepsilon_r(0, \lambda) = 0$ for 0 greater than a critical value. However, it does appear that if one replaces $r_r(0, \lambda)$ and $r_c(0, \lambda)$ with hemispherical values in the denominators of our equations (11) and (12), one can obtain equation

(6) of Landro and McCormick. It does not seem likely, therefore, that their approximations lead to serious errors if multiple reflections are unimportant.

Another approximation often made is to set the cover temperature T_c equal to the air temperature. An inspection of equation (12) shows that this is a good approximation if the cover emissivity can be neglected and $h_{ca} \gg h_{rc}$.

4. ESTIMATES OF REQUIRED SPECTRAL PROPERTIES

In order to evaluate the equations formulated in the previous section it is necessary to estimate the spectral and angular dependences of the thermal sky radiance and of the properties of the radiator and cover. A simple model of sky radiance will be discussed which produces estimates of $\varepsilon_s(0, \lambda)$ when only the non-spectral hemispherical value ε_s is available. In a similar spirit we develop a simple technique for estimating the optical properties of the (polyethylene) cover based on the spectral transmittance at normal incidence. A similar technique is used to estimate the optical parameters of a radiator consisting of an aluminized plastic film based on the measured spectral reflectance at normal incidence.

4.1. *Model for thermal sky radiance*

The most accessible measure of thermal sky radiance is the total hemispherical sky emissivity ε_s obtained from pyrgeometer readings. Even this data is often not reported in conjunction with measurements of radiative cooling. For clear nighttime conditions a reliable estimate of ε_s can be made using the correlation with ambient dewpoint temperature discussed in the Introduction. Irrespective of the source of the value for the total sky emissivity, it is desired to utilize ε_s to estimate the full function $\varepsilon_s(0, \lambda)$. This quantity has been measured by our group in six U.S. locations over a two year period. Based on a preliminary analysis of several summer months of data at three locations (Gaithersburg, St. Louis, and Tucson), the angular and spectral sky emissivity is given approximately by the following model:

The spectral and angular dependence of $\varepsilon_s(\lambda, 0)$ are separated in a simple way. The *hemispherical* spectral sky emissivity is given by

$$\varepsilon_s(\lambda) = 2\int_0^1 \mathrm{d}\cos\theta\cos\theta\,\varepsilon_s(\lambda, \theta).$$

We assume that the deviation of $\varepsilon_s(\lambda)$ from unity is proportional to an effective atmospheric transparency, $t_s(\lambda)$, as expressed in the form

$$\varepsilon_s(\lambda) = 1-(1-\varepsilon_s)(t_s(\lambda)/\bar{t}_s). \tag{13}$$

Here the 'transparency' function $t_s(\lambda)$ shown in Fig. 1 is different from zero only within the 8–13 μm window. It is based on computed clear sky radiances for typical midlatitude-summer values of atmospheric temperature and moisture [7]. The parameter $\bar{t}_s$ is determined from the normalization condition

$$\int_0^\infty \mathrm{d}\lambda\,\varepsilon_s(\lambda)B_a(\lambda) = \varepsilon_s\int_0^\infty \mathrm{d}\lambda\,B_a(\lambda),$$

which follows from equation (6). Equation (13) can now be generalized to include the angular dependence of the radiation,

$$\varepsilon_s(\lambda, \theta) = 1-(1-\varepsilon_s)[t_s(\lambda)/\bar{t}]C\,\mathrm{e}^{-bm}, \tag{14}$$

where $m = 1/\cos\theta$ is the air mass and C is a constant to assure normalization. The best value of b for use in

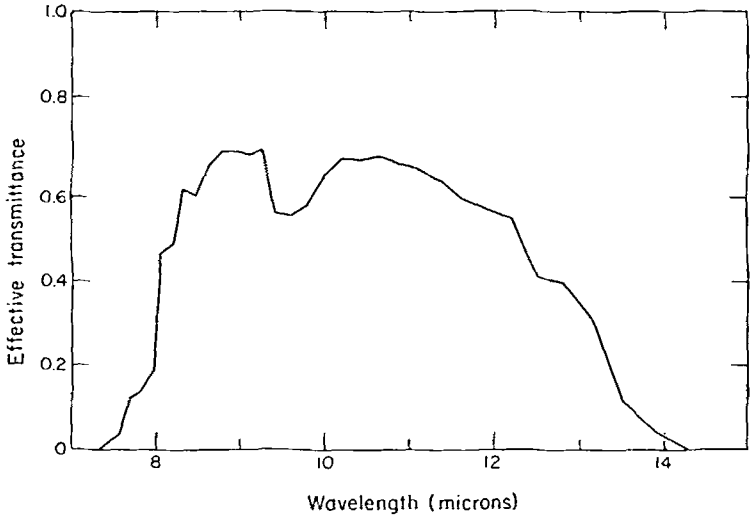

FIG. 1. Effective spectral transmittance of the atmosphere (vertical path, midlatitude-summer atmosphere). These values have been obtained by requiring that the computed sky radiance $R_s(\theta, \lambda)$ given by equations (5) and (14) agree with the calculated values given in [7] for $\theta = 0$. Assumptions in ref. [7] included air and dewpoint temperatures of 21 and 16°C, respectively, and no clouds. This transmittance is approximately equal to the actual transmittance except in the ozone absorption bands between 9.4 and 9.9 μm.

equation (14) is the subject of an ongoing study. For this paper we have used

$$b = 1.7\varepsilon_s - 1.1 \quad \text{for} \quad 0.75 \leqslant \varepsilon_s \leqslant 1. \tag{15}$$

For the range of b of importance here (0.1–0.6), C is given with an accuracy of a few percent by

$$C = e^{1.7b}.$$

Equation (14) is useful for (average) cloudy conditions as well as clear. One important limitation of the equation is that values smaller than 0.75 for ε_s lead to negative values for $\varepsilon_s(\lambda, 0)$, indicating a breakdown of our approximations. For clear skies and dewpoint temperatures below about 0°C, for which $\varepsilon_s < 0.75$, the shape function $t_s(\lambda)$ would have to be changed substantially. In particular, a secondary window opens $[t_s(\lambda) \neq 0]$ in the spectral range 17–22 μm.

4.2. *Optical properties of plastic films used as windscreens and radiators*

If the real and imaginary parts of the complex index of refraction were known across the thermal infrared spectrum it would be a straightforward if lengthy task to compute the optical properties of plastic films used as radiators and windscreen covers. Unfortunately, this complete information does not appear to exist and we must consequently infer values of the optical constants from measured transmission and reflection spectra.

The general approach for the determination of optical constants is as follows. The real part of the index of refraction will be taken as a constant (*ca.* 1.5), which represents the actual index of refraction outside absorption bands. The imaginary part of the index of refraction will be determined by an optical transmission or reflection measurement. This approach is reasonable provided the absorption in the plastic is not extremely strong. Interference effects will be neglected. For windscreen optical properties, the normal spectral transmittance will be used as input data, thus ensuring that the computed normal transmittance is not influenced by the above assumptions. Thus the errors introduced by the assumptions have been limited. Likewise, for the radiator (aluminized PVF), the normal spectral reflectance is used to determine the optical properties, ensuring that the accuracy of the spectral normal emissivity is limited only by the accuracy of measurement. A similar approach has been used by Clark and Blanpied [25].

The Fresnel reflectance for a single air–plastic interface is [31, 32]

$$\mathscr{R}(0) = \frac{1}{2}\left[\frac{\cos 0' - n\cos 0}{\cos 0' + n\cos 0}\right]^2 + \frac{1}{2}\left[\frac{\cos 0 - n\cos 0'}{\cos 0 + n\cos 0'}\right]^2 \tag{16}$$

where $0'$ is the angle of incidence inside the medium with index of refraction n as given by Snell's law:

$$n\sin 0' = \sin 0. \tag{17}$$

Equation (16) is an average over parallel (first term) and perpendicular (second term) polarizations. (Parallel here means that the electric field of the incident wave is parallel to the plane of incidence.)

In terms of the Fresnel reflectance, the transmissity of the windscreen cover can be obtained after accounting for multiple reflections,

$$t_c(0,\lambda) = [1-\mathscr{R}(0)]^2 \exp\left[\frac{-\alpha(\lambda)d}{\cos 0'}\right] \left\{1-\mathscr{R}^2(0)\exp\left[\frac{-2\alpha(\lambda)d}{\cos 0'}\right]\right\}^{-1} \tag{18}$$

where $\alpha(\lambda)$ is the spectral absorption coefficient and d is the film thickness. Since measured values of $t_c(0,\lambda)$ are available, this equation can be inverted to obtain values of $\alpha(\lambda)d$, which can then be employed to find $t_c(0,\lambda)$ for $0 \neq 0$. [The solution for $\alpha(\lambda)d$ can usually be simplified by means of the relation $\mathscr{R}^2(0) \ll 1$.] The emissivity of the cover is given by

$$\varepsilon_c(0,\lambda) = [1-\mathscr{R}(0)]\left\{1-\exp\left[\frac{-\alpha(\lambda)d}{\cos 0'}\right]\right\} \times \left\{1-\mathscr{R}(0)\exp\left[\frac{-\alpha(\lambda)d}{\cos 0'}\right]\right\}^{-1}, \tag{19}$$

which can also be evaluated once $\alpha(\lambda)d$ is known. The reflectance of the windscreen cover can be obtained from an equation analogous to (18) and (19) or from the relation $r+\varepsilon+t = 1$.

For the case in which the radiator is an aluminized plastic film, the optical properties can be determined by a method similar in spirit to that used for the windscreen, but different in detail. We assume the reflectance of the aluminum film is unity, and that the Fresnel reflectance (16) applies to the upper surface. The overall radiator reflectance is then

$$r_r(0,\lambda) = \mathscr{R}(0) + [1-\mathscr{R}(0)]^2 \exp\left[\frac{-2\alpha(\lambda)d}{\cos 0'}\right] \times \left\{1-\mathscr{R}(0)\exp\left[\frac{-2\alpha(\lambda)d}{\cos 0'}\right]\right\}^{-1}. \tag{20}$$

Since it is assumed that $r_r(0,\lambda)$ is measured, $\alpha(\lambda)d$ can be determined which, in turn, specifies $r_r(0,\lambda)$ for $0 \neq 0$. Since the radiator is opaque, the spectral emissivity is determined from the relationship $\varepsilon_r(0,\lambda) = 1-r_r(0,\lambda)$.

Another approach to determine the thermal optical properties of plastic films has been suggested by Tien *et al.* [33], and applied by Rubin [34]. The thermal spectrum is divided into about five parts ("bands"), and the spectral optical constants are replaced by suitable averages within each band. This procedure has some significant shortcomings, however, whenever the optical constants vary within a band. The derived approximate equations for a single band obey Beer's law (the exponential decay of radiation with distance) whereas multichromatic radiation in a medium with spectrally variable optical constants does not obey Beer's law. We therefore believe that the more complex

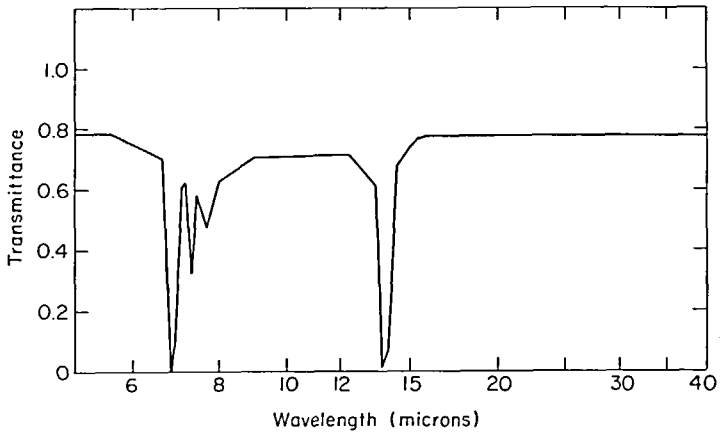

FIG. 2. Normal spectral transmittance of a 50 μm polyethylene film.

method outlined in this section is preferable for the evaluation of thermal infrared optical properties.

5. NUMERICAL RESULTS

The mathematical description of a radiator panel given in the last two sections was solved numerically for net cooling power for several interesting cases. Spectrally selective and nonselective radiators were simulated, and the sensitivity of the solutions to parametric variations was examined.

In all cases the windscreen or cover was a 50 μm (2 mil) polyethylene film. The normal spectral transmittance of this film is shown in Fig. 2, as digitized for the computer integrations. Figure 3 shows three independent measurements of the spectral reflectance of aluminized 12 μm ($\frac{1}{2}$ mil) polyvinyl fluoride (PVF). Curves A and B have both been used in our calculations. Curve A is due to Catalanotti *et al.* [6] as digitized by us and curve B is from our own measurements. Curve C is from the paper by Michell and Biggs [20]. Most of the differences shown are probably due to measurement techniques rather than sample differences. The difference between curves B and C in the neighborhood of 25 μm is rather large and may therefore be due to sample differences. Landro and McCormick [17] report values for the hemispherical spectral reflectance of a similar sample measured by Christie. They give a value of about 35% between 21 and 25 μm, which falls between curves B and C.

The non-radiative heat transfer coefficients required in equations (11) and (12) were estimated using standard engineering formulae [35, 36], in accordance with the dimensions of our radiator panels. The values are summarized in Table 1.

Equation (12) is solved for the cover temperature, and then equation (11) is used to calculate the net cooling power N. The integrations over wavelength are performed in steps of 0.1 μm wavelength, and the integrations over zenith angle proceed in steps of 3°. Results for the 12 μm aluminized PVF as a radiator are shown in Fig. 4. Curves A and B correspond to the spectral reflectances of Fig. 3. For comparison, the cooling power of a blackbody with the same polyethylene windscreen is also shown. The atmospheric conditions assumed are $\varepsilon_s = 0.82$, $T_a = 300$ K,

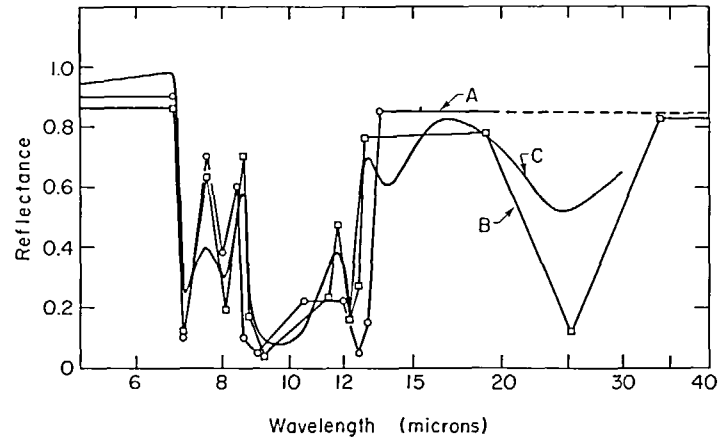

FIG. 3. Normal spectral reflectance of an aluminized polyvinyl fluoride film 12 μm thick. Curves A and C are from refs. [6] and [20].

Table 1. Non-radiative heat transfer coefficients

Heat transfer coefficient	Symbol	Heat flow direction	Value ($W m^{-2} K^{-1}$)	Remarks
Radiator-to-air (back losses)	h_{ra}	↑↓	0.3	10 cm plastic foam
Radiator-to-cover	h_{rc}	↓	0.9	2.7 cm air gap
	h_{rc}	↑	$1.3(T_r-T_c)^{1/4}$	laminar convection T_r-T_c in °C
Cover-to-air	h_{ca}	↑↓	5.4	forced convection with windspeed of 2 m s^{-1} length scale = 1 m
	h_{ca}	↑↓	17	forced convection with windspeed of 10 m s^{-1}

windspeed = 2m s^{-1}. The corresponding sky temperature depression is 14.5°C, a typical value for clear skies (dewpoint temperature about 13°C). The difference in cooling power between curves A and B gives an estimate of the importance of errors present in the spectral reflectance data. Large intercepts on a plot of this type are associated with high radiator emissivity within the atmospheric window. The steeper (negative) slopes on the plot, are caused by a larger overall thermal emissivity. The reasons for this behavior can be seen by an inspection of equation (7).

It is useful for many purposes to plot panel cooling performance in a non-dimensional fashion. Figures 5 and 6 show numerical results for the aluminized 12 μm PVF film (spectrum A) plotted as efficiency vs dimensionless temperature difference

$$\tau = \frac{4(T_a - T_r)}{(1-\varepsilon_s)T_a}.$$

These figures also show the computed sensitivity to variations in air temperature, windspeed, and sky emissivity. The effect of wind merely alters the

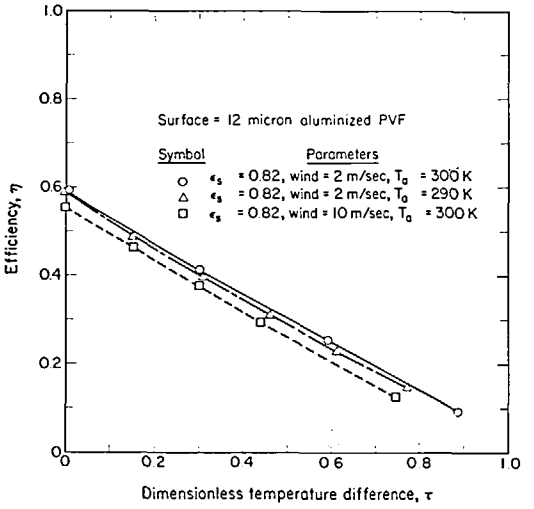

FIG. 5. Computed sensitivity of cooling efficiency to changes in air temperature and wind speed. Spectral data used are shown as curve A in Fig. 3.

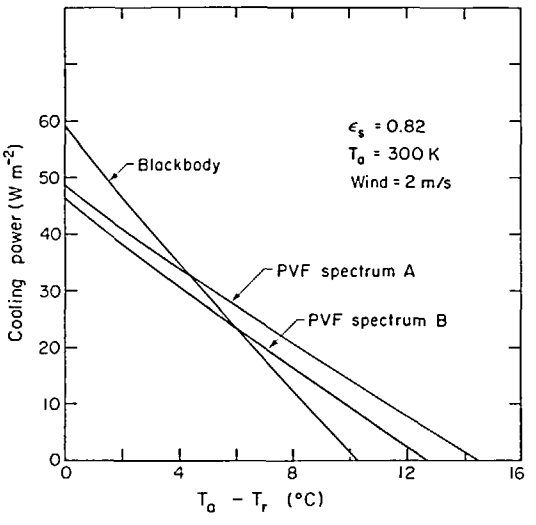

FIG. 4. Computed cooling power produced by three radiators below a polyethylene windscreen 50 μm thick, as a function of the air temperature minus radiator temperature (ε_s = 0.82, T_a = 300 K, wind = 2 m s^{-1}).

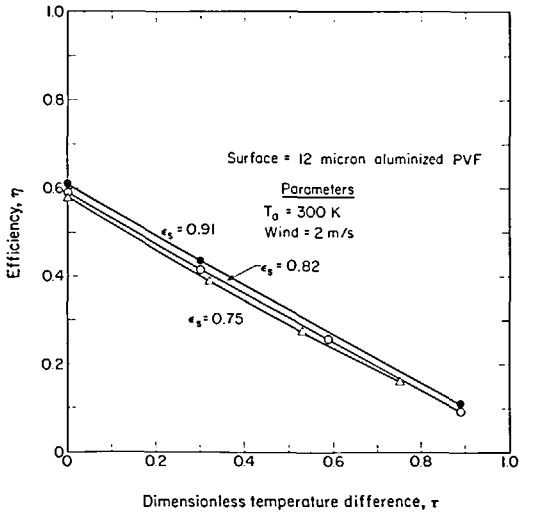

FIG. 6. Computed sensitivity of cooling efficiency to changes in the sky emissivity. Spectral data used are shown as curve A in Fig. 3.

windscreen convection coefficient in the computer model. Of course, in an experiment, the effect of wind can be much greater if it causes the windscreen to move. The relative insensitivity of the plots of η vs τ to changes in atmospheric conditions suggests that experiments to determine performance of panels need only determine the slope and intercept of such a plot. Such a determination is analogous to the standard efficiency plots for solar panels [37].

6. SELECTED EXPERIMENTAL RESULTS

We shall review measurements of cooling rates by Landro and McCormick [17] and then report selected measurements of our own.

Landro and McCormick reported measurements of cooling rates of 12 μm aluminized PVF beneath a thin (12 μm) polyethylene cover. This apparatus was insulated on the sides and back with 5 cm of polystyrene foam. The sample area was only 0.01 m^2. Edge effects complicate the interpretation of their results, but they showed clearly that PVF can produce lower temperatures than a black painted surface. The results for PVF (from their Fig. 8) have been replotted here in Fig. 7. The sky emissivity was estimated by the use of equation (2) based on the reported values of absolute humidity converted to dewpoint temperature. Note that the data measured at different values of dewpoint fall on the same curve. Thus the procedure of plotting η vs τ has eliminated the sky emissivity dependence of the results. Also noteworthy is the fact that the apparent efficiencies exceed unity. The reason for this contradictory aspect of the data is not clear. However, the substantial edge effects offer a possible explanation.

Our measurements for 12 μm aluminized PVF and white paint radiators were performed with our radiative cooling panel test facility [28, 29]. The radiators are 53 cm wide and 94 cm long. Both radiators were covered with a 50 μm thick polyethylene film suspended 2.7 cm above the radiators. The thickness of the plastic foam insulation on the back and sides is 10 cm. The sky emissivity was monitored using an Eppley pyrgeometer. We estimate the accuracy of the pyrgeometer measurement to be 0.02 emissivity units. Due to the relatively large size of our radiator plates, the view factor correction is small. The gross radiating area is 0.506 m^2, and the net effective area, after allowance for blocking of the sky at the radiator edges, is 0.474 m^2. During the measurements the heater power was held fixed for 120 min, and then changed by a nominal 20 W m^{-2}. The difference between temperature depressions $T_a - T_r$ achieved on heating and cooling was used as a measure of the departure from thermal equilibrium at the end of the 120 min period. Thus for the PVF panel, temperature depressions $T_a - T_r$ were increased by 0.6°C if the experimental point was reached by cooling (after a reduction in heater power), and decreased by a like amount if the point was reached by warming. The corresponding correction for the white-painted radiator was 0.3°C. These values are consistent with the known radiator heat capacities and emissivities.

The results of the measurements are shown in Fig. 8, where they are compared with numerical results. For the calculations pertaining to white paint, the normal emissivity was taken equal to 0.9, independent of wavelength. For the calculations pertaining to the PVF radiator, spectrum B in Fig. 3 was employed. For the numerical calculations, uncertainties in the spectral emissivities of the radiators are probably the most significant errors. For the experimental results, uncertainty in the measured sky emissivity is probably the most significant error. In general the agreement of the experiment with the calculated results is quite good, within the uncertainties known to be present. Since the measurements were obtained on the same night for the data shown, the comparative results for PVF vs white

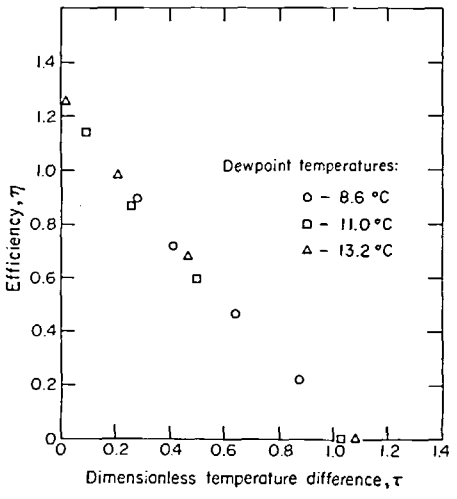

FIG. 7. Performance curve based on ref. [17]. Measured values of cooling efficiency as a function of dimensionless temperature difference for an aluminized PVF radiator with a 12 μm polyethylene cover.

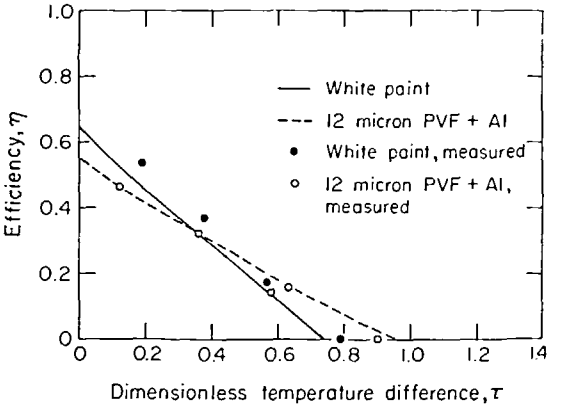

FIG. 8. Comparison of measured and calculated cooling efficiencies for a surface painted white and for a 12 μm aluminized PVF radiator. During these measurements the air temperature was in the range 22 ± 1°C, the dewpoint temperature was 0 ± 1°C, and the sky emissivity was 0.73 ± 0.01. The low point (open circle at $\tau = 0.58$) was probably caused by wind-induced motion of the polyethylene cover. Spectral data used for the PVF radiator is curve B in Fig. 3.

paint are not affected by the measurement uncertainties in the sky emissivity. Whereas the computer model shows a crossover (equal efficiencies) at $\tau \approx 0.36$, the data indicate a crossover at roughly $\tau = 0.55$. This result shows that the white paint is a better radiator relative to PVF than one might believe based on the radiator emissivities we have used. The discrepancy could be due to the uncertainty in the optical constants of PVF (Fig. 3), but it could also be due to the incorrectness of the grey-body assumption $\varepsilon_r(0, \lambda) = 0.9$ for the white paint. Measured values of the diffuse spectral reflectance for white paint with titanium dioxide pigment [20, 38] suggest that $\varepsilon_r = 0.9$ within the 8–13 μm atmospheric window, but that $\varepsilon_r \approx 0.8$ outside this window. Thus the white paint may exhibit a weak spectral selectivity which improves performance. In any case it is clear that 12 μm aluminized PVF, often used as a selective radiator, is superior to simple white paint only at the lowest radiator temperatures. This result is in agreement with the work of Michell and Biggs, who showed that at about 5°C below air temperature (and $T_a = 283$ K, $\varepsilon_s = 0.804$, which implies $\tau = 0.36$) a white-painted surface produced more cooling than a PVF surface.

7. CONCLUSIONS

The heat transfer within radiative cooling panels can be understood on the basis of the equations presented in this paper. The good agreement between numerical calculations and measurements confirms that all the significant heat transfer mechanisms have been taken into account.

The efficiency for radiative cooling defined in Section 2 is a useful figure of merit. In particular, plots of efficiency vs a dimensionless temperature difference can be prepared which are analogous to standard efficiency plots for solar collectors.

Selective radiators fabricated from 12 μm aluminized PVF are unable to outperform titanium dioxide based white paint, except at the lowest temperatures. The primary reason for this failure is the departure of the radiator infrared optical properties from the ideal. Better selective radiators should be developed.

Acknowledgements—Computer programming for and some early experiments with the radiator test facility were performed by Mark Kruskopf [29]. The computer program for computing the optical properties of radiators and windscreens and integrating the heat transfer equations was written by Mark Sobolewski [29]. Steve Kanzler and Dave Evans also made significant contributions. This work was supported by the Assistant Secretary for Conservation and Renewable Energy, Office of Solar Heat Technologies, Passive and Hybrid Solar Energy Division of the U.S. Department of Energy under Contract No. DE-AC03-76 SF00098.

REFERENCES

1. H. R. Hay and J. I. Yellot, Natural air-conditioning with roof ponds and movable insulation, *ASHRAE Jl* **75**, 165–177 (1969).
2. J. I. Yellot and H. R. Hay, Thermal analysis of buildings with natural air-conditioning, *ASHRAE Jl* **75**, 178–190 (1969).
3. J. T. Bliss, The performance of an experimental system using solar energy for heating and night radiation for cooling a building, *Proc. UN Conf. on New Sources of Energy*, Vol. 5, pp. 148–158, Rome (1964).
4. A. K. Head, Australian patent 239364 (1959), Method and means for producing refrigeration by selective radiation. U.S. patent 3043112 (1962).
5. F. Trombe, Perspectives sur l'utilisation des rayonnements solaries et terrestres dan certain regions du monde, *Rev. Gén. Thermique* **6**, 1285–1314 (1967).
6. S. Catalanotti, V. Cuomo, G. Piro, D. Ruggi, V. Silvestrini and G. Troise, The radiative cooling of selective surfaces, *Solar Energy* **17**, 83–89 (1975).
7. P. Berdahl and R. Fromberg, The thermal radiance of clear skies, *Solar Energy* **29**, 299–314 (1982).
8. P. Grenier, Refrigeration radiative: effect de serre inverse, *Rev. Phys. Appl.* **14**, 87–90 (1979).
9. S. E. Golli and P. Grenier, Effect de serre inverse—application a une cave solaire, *J. Phys.* **42**, C1-431–C1-436 (1981).
10. B. Bartoli, S. Catalanotti, B. Coluzzi, V. Cuomo, V. Silvestrini and G. Troise, Nocturnal and diurnal performance of selective radiators, *Applied Energy* **3**, 267–286 (1977).
11. A. Addeo, R. Monza, M. Peraldo, B. Bartoli, B. Coluzzi, V. Silvestrini and G. Troise, Selective covers for natural cooling devices, *Il Nuovo Cimento* **1C**, 419–429 (1978).
12. A. Addeo, L. Nicolais, G. Romeo, B. Bartoli, B. Coluzzi and V. Silvestrini, Light selective structures for large scale air conditioning, *Solar Energy* **24**, 93–98 (1980).
13. A. Andretta, B. Bartoli, B. Coluzzi and V. Cuomo, Selective surfaces for natural cooling devices, *J. Phys.* **42**, C1-423–C1-430 (1981).
14. C. G. Granqvist and A. Hjortsberg, Radiative cooling to low temperatures: general considerations and application to selectively emitting SiO films, *J. Appl. Phys.* **52**, 4205–4220 (1981).
15. A. Hjortsberg and C. G. Granqvist, Radiative cooling with selectively emitting ethylene gas, *Appl. Phys. Lett.* **39**, 507–509 (1981).
16. C. G. Granqvist, A. Hjortsberg and T. S. Ericksson, Radiative cooling to low temperatures with selectively emitting surfaces, in *Proc. Int. Solar Energy Congress*, Brighton, 1981 (Edited by D. O. Hall and J. Morton) Vol. 1, pp. 562–566. Pergamon Press, Oxford (1982).
17. B. Landro and P. G. McCormick, Effect of surface characteristics and atmospheric conditions on radiative heat loss to a clear sky, *Int. J. Heat Mass Transfer* **23**, 613–620 (1980).
18. B. Landro and P. G. McCormick, Application of nocturnal convective and radiative cooling for air conditioning—performance of an experimental system, in *Proc. Int. Solar Energy Congress*, Brighton, 1981 (Edited by D. O. Hall and J. Morton) Vol. 1, pp. 567–572. Pergamon Press, Oxford (1982).
19. D. Michell, Selective radiative cooling—another look, Report 62/SS of the CSIRO Div. of Tribophysics, University of Melbourne, Australia (1976).
20. D. Michell and K. L. Biggs, Radiative cooling of buildings at night, *Applied Energy* **5**, 263–275 (1979).
21. B. Givoni, Passive cooling of buildings—options and evaluation, in *Proc. Int. Solar Energy Congress*, Brighton, 1981 (Edited by D. O. Hall and J. Morton) Vol. 3, pp. 1783–1791. Pergamon Press, Oxford (1982).
22. E. Hernandez and E. Mayer, Nocturnal infrared radiative cooling experiments in Mexico, in *Solar Technology for Building* (Edited by C. Stambolis) Vol. 2, pp. 428–436. RIBA, London (1978).
23. A. W. Harrison, Effect of atmospheric humidity on radiative cooling, *Solar Energy* **26**, 243–248 (1981).

24. T. E. Johnson, Radiation cooling of structures with infrared transparent windscreens, *Solar Energy* **17**, 173–178 (1975).
25. G. Clark and M. Blanpied, The effect of IR transparent windscreens on net nocturnal cooling from horizontal surfaces, in *Proc. 4th National Passive Solar Conf.*, Kansas City, 1979 (Edited by G. Franta) Vol. 4, pp. 509–513. Amer. Sec. of the Int. Solar Energy Society, Newark, Delaware, U.S.A. (1979).
26. R. Manning, G. Clark, J. Rudzki and M. Blanpied, Measurements and simulations of radiative cooling through IR transparent windscreens, in *Proc. 5th National Passive Solar Conf.*, Amherst, U.S.A. 1980 (Edited by J. Hayes and R. Snyder) Vol. 5.2, pp. 717–721. Amer. Sec. of the Int. Solar Energy Society, Newark, Delaware, U.S.A. (1980).
27. G. R. Conrad, G. T. Pytlinski and T. C. McConnell, Assessment of contemporary residential roof surfaces as nocturnal radiators and solar collectors, in *Proc. Int. Passive and Hybrid Cooling Conf.*, Miami Beach, U.S.A., 1981 (Edited by A. Bowen, E. Clark and K. Labs) pp. 251–255. Amer. Sec. of the Int. Solar Energy Society, Newark, Delaware, U.S.A. (1981).
28. F. Sakkal, M. Martin and P. Berdahl, Experimental facility for selective radiative cooling surfaces, in *Proc. 4th National Passive Solar Conf.*, Kansas City, 1979 (Edited by G. Franta) Vol. 4, pp. 483–487. Amer. Sec. of the Int. Solar Energy Society, Newark, Delaware, U.S.A. (1981).
29. M. S. Kruskopf, P. Berdahl, M. Martin, F. Sakkal and M. Sobolewski, Radiative cooling test facility and performance evaluation of 4 mil aluminized polyvinyl fluoride and white paint surfaces, Univ. of California, Lawrence Berkeley Laboratory Report LBL-12049 (1980).
30. W. C. Miller and J. O. Bradley, Radiative cooling with selective surfaces in a desert climate, in *Proc. 4th National Passive Solar Conf.* 4, 480–482 (1979). See ref. [25].
31. O. S. Heavens, *Optical Properties of Thin Solid Films*, Sec. 4.2. Butterworths, London (1955); Dover, New York (1965).
32. D. K. Edwards, *Radiation Heat Transfer Notes*, Sec. 2.F. Hemisphere, New York (1981).
33. C. L. Tien, C. K. Chan and G. R. Cunningham, Infrared radiation of thin plastic films, *J. Heat Transfer* **94**, 41–45 (1972).
34. M. Rubin, Infrared properties of polyethylene terephthalate films, *Solar Energy Materials* **6**, 375–380 (1982).
35. F. Kreith, *Principles of Heat Transfer*. Harper & Row, New York (1973).
36. M. Jacob, *Heat Transfer*. Wiley, New York (1949).
37. Methods of testing to determine the thermal performance of solar collectors, ASHRAE Standard 93–77, Amer. Soc. for Heating, Refrigeration, and Air-Conditioning Engineering, New York (1977).
38. Y. S. Touloukian, D. P. DeWitt and R. S. Hernicz, *Thermal Radiative Properties: Coatings*. Vol. 9, p. 219. IFI/Plenum Press, New York (1972).

PERFORMANCES THERMIQUES DES PANNEAUX A REFROIDISSEMENT RADIATIF

Résumé—Les performances de panneaux qui se refroidissent par rayonnement infrarouge vers le ciel sont calculés à partir des principes fondamentaux. On définit l'efficacité d'un tel panneau. Des calculs numériques sur les équations complètes de transfert thermique sont effectués pour des surfaces horizontales avec des couvertures transparentes pour l'infrarouge. Des graphiques d'efficacité en fonction d'une différence de température adimensionnelle montrent l'insensibilité aux variations de la température d'air, de la vitesse du vent et de la luminance du ciel, comme pour les courbes d'efficacité des panneaux solaires. Des mesures expérimentales montrent que, pour la plupart des applications, la peinture blanche est meilleure que le film de polyvinyl aluminisé.

THERMISCHE LEISTUNG VON ABSTRAHLENDEN KÜHLFLÄCHEN

Zusammenfassung—Die Leistung von Kühlflächen, welche durch infrarote Abstrahlung Wärme an den Himmel abgeben, wird nach den Grundgleichungen berechnet. Der Wirkungsgrad einer abstrahlenden Kühlfläche wird definiert. Numerische Berechnungen mit allen Wärmeübergangsgleichungen wurden für horizontale Oberflächen im infraroten Bereich mit transparenten Abdeckungen durchgeführt. Es wird gezeigt, daß Darstellungen, welche den Wirkungsgrad in Abhängigkeit von einer dimensionslosen Temperaturdifferenz zeigen, unempfindlich gegen Veränderungen der Umgebungstemperatur, der Windgeschwindigkeit und der Himmelsstrahlung sind, und damit zu Auftragungen führen, die den normalen Wirkungsgradkurven von Sonnenkollektoren gleichen. Versuche zeigten, daß für die meisten Anwendungen weiße Farbe ein besseres Strahlungsverhalten zeigt als eine aluminiumbedampfte Polyvinylfluorid-Folie.

ТЕПЛОВЫЕ ХАРАКТЕРИСТИКИ РАДИАЦИОННЫХ ОХЛАЖДАЮЩИХ ПАНЕЛЕЙ

Аннотация—Исходя из первых принципов, проведен расчет характеристик панелей, осуществляющих охлаждение за счет теплоотдачи инфракрасным излучением в окружающую среду. Определена эффективность таких панелей. Используя полные уравнения теплопереноса, проведены расчеты на ЭВМ для горизонтальных поверхностей с покрытиями, прозрачными для инфракрасного излучения. Показано, что кривая зависимости эффективности панели от безразмерной разности температур нечувствительна к изменениям температуры воздуха, скорости ветра и яркости неба и аналогична стандартным кривым эффективности солнечных панелей. Экспериментальные измерения показывают, что в большинстве случаев панель, окрашенная белой краской, излучает больше тепла, чем панель, покрытая алюминированной полифторвиниловой пленкой.